Estuarine, Coastal and Shelf Science 167 (2015) 125–137

Contents lists available at ScienceDirect

Estuarine, Coastal and Shelf Science

journal homepage: www.elsevier.com/locate/ecss

Using bio-optical parameters as a tool for detecting changes in the phytoplankton community (SW Portugal)

Priscila C. Goela [a, b, *], John Icely [a, c], Sónia Cristina [a, b], Sergei Danchenko [a, b], T. Angel DelValls [b], Alice Newton [a, d]

[a] CIMA, Universidade do Algarve, Campus de Gambelas, 8005-139 Faro, Portugal
[b] Facultad de Ciencias del Mar y Ambientales – Universidad de Cadiz, Campus de Puerto Real, Polígono San Pedro s/n, Puerto Real, 11510 Cadiz, Spain
[c] Sagremarisco Lda., Apartado 21, 8650–999 Vila do Bispo, Portugal
[d] NILU-IMPEC, Box 100, 2027 Kjeller, Norway

ARTICLE INFO

Article history:
Received 30 September 2014
Received in revised form
23 July 2015
Accepted 29 July 2015
Available online 1 August 2015

Keywords:
Phytoplankton
Absorption coefficient
Algal blooms
HPLC
Iberian Peninsula
Sagres

ABSTRACT

Upwelling events off the Southwest coast of Portugal can trigger phytoplankton blooms that are important for the fisheries and aquaculture sectors in this region. However, climate change scenarios forecast fluctuations in the intensity and frequency of upwelling events, thereby potentially impacting these sectors. Shifts in the phytoplankton community were analysed from the end of 2008 until the beginning of 2012 by examining the bio-optical properties of the water column, namely the absorption coefficients for phytoplankton, non-algal particles and coloured dissolved organic matter (CDOM). The phytoplankton community was assessed by microscopy, with counts from an inverted microscope, and by chemotaxonomic methodologies, using pigment concentrations determined by High-Performance Liquid Chromatography (HPLC). Results both from microscopy and from chemotaxonomic methods showed a shift from diatom dominance related to bloom conditions matching upwelling events, to small flagellate dominance related to no-bloom conditions matching relaxation of upwelling. During bloom conditions, light absorption from phytoplankton increased markedly, while non-algal particles and CDOM absorption remained relatively constant. The dynamics of CDOM in the study area was attributed to coastal influences rather than from phytoplankton origin. Changes in phytoplankton biomass and consequent alterations in phytoplankton absorption coefficients were attributed to upwelling regimes in the area. Bio-optical parameters can contribute to environmental monitoring of coastal and oceanic waters, which in the case of the European Union, involves the implementation of the Water Framework, Marine Strategy Framework and Marine Spatial Planning Directives.

1. Introduction

Phytoplankton is the basis of most of the marine food web, thus the knowledge of the dynamics of its communities is crucial for understanding shifts in the marine ecosystems. Temporary proliferations of phytoplankton, known as “blooms”, are common and natural in coastal environments [Cullen (2008)] and are often due to the nutrient enrichment of the system, either by terrestrial runoff or by wind induced upwelling events. Indeed, areas where these events occur recurrently are known to be among the most productive areas of the world [Smith and Hollibaugh (1993), Loureiro et al. (2008)], and support economically important industries for fisheries and offshore aquaculture (e.g). [Kifani et al. (2008), Rueda-Roa and Muller-Karger (2013)]. However, some phytoplankton blooms can produce undesirable effects such as inducing high mortalities in fish and other marine species, contaminating seafood by algal toxins, and even directly damaging human health, thereby impacting human activities and welfare in the surrounding area [Hu et al. (2014)]. These events are referred to as Harmful Algal Blooms (HABs) and they can be caused either by an excessive proliferation of a specific phytoplankton species, or by those species that produce toxins. Thus, the need for an effective and global monitoring of phytoplankton algal blooms becomes

* Corresponding author. CIMA, Universidade do Algarve, Campus de Gambelas, 8005-139 Faro, Portugal.
E-mail addresses: prgoela@ualg.com, priscila.goela@gmail.com (P.C. Goela), john.icely@gmail.com (J. Icely), cristina.scv@gmail.com (S. Cristina), danchenko-sergei@tut.by (S. Danchenko), angel.valls@uca.es (T. Angel DelValls), anewton@ualg.pt (A. Newton).

http://dx.doi.org/10.1016/j.ecss.2015.07.037

evident for ocean management.

The classical studies and monitoring of phytoplankton blooms are based on discrete sampling schemes in limited areas, followed by intensive and laborious laboratory analysis such as identification and counts of phytoplankton by inverted microscopy. More recently, instrumental techniques such as High-Performance Liquid Chromatography (HPLC) and flow cytometry provide useful data to characterise the phytoplankton community in a more rapid and automated way, especially when combined with computational approaches [e.g. CHEMTAX, Mackey et al. (1996)]. The results of these techniques also allow the assessment of the functional diversity of small cell phytoplankton communities (nano- and picoplankton), that are normally classified as unidentified flagellates by the conventional light microscopy technique. This knowledge becomes more relevant since several climate change scenarios forecast a shift in domination from diatoms to smaller flagellates [e.g. Bopp et al. (2005), Leterme et al. (2008)], thereby modifying ecosystem function [Beaugrand (2005), David et al. (2012)]. This theme is relevant in the context of the implementation of the European Union's Water Framework Directive (WFD, [EC (2000)]), Marine Strategy Framework Directive (MSFD, [EC (2008)]), and the Marine Spatial Planning Directive (MSPD, [EU (2014)]), particularly, with regard to the choice of appropriate plankton indicators and metrics used to define the environmental status of the water masses. For example, Garmendia et al. (2013) recognize that the assessment of eutrophication for the WFD is based on only a limited number of indicators, particularly total chlorophyll *a* (TChl*a*) concentration, for which the data is readily available. However, Domingues et al. (2008) warn about using only TChl*a* for the implementation of WFD, especially in areas where nano and picoplankton are important components of the community. Even when composition-based indicators are used to evaluate the ecosystem function [Devlin et al. (2007, 2009)], these only include diatoms, dinoflagellates, and microflagellates (e.g *Phaeocystis* sp.). It is notable that the idea of a shift between diatom to flagellate dominated communities is explicitly considered by the MSFD, i.e. the relative proportions of diatoms and flagellates should be evaluated for Indicator 5.2.4 in Descriptor 5 for Eutrophication [EC (2008)]. In this context, the use of chemotaxonomic methods in combination with the classical methods would be useful to evaluate and characterise Descriptor 5.

Remote sensing of ocean colour is also a powerful tool for monitoring phytoplankton communities, because of its extensive spatial and temporal coverage, and is considered as the best option for observing extensive coastal and oceanic blooms, especially, when the observations are supplemented by direct sampling [Johnsen et al. (1997), Tangen (1997), Cullen (2008)]. Remote sensors estimate chlorophyll biomass by using reflectance ratio algorithms, which strongly indicate that chlorophyll biomass is related to oceanic absorption bio-optical properties [Gordon et al. (1983), O'Reilly et al. (1998), Lyon et al. (2004)]. These algorithms are based on the radiative transfer model [Preisendorfer (1971)], which relates the sea surface reflectance with the absorption and scattering processes in the water column. In addition to the absorption properties of pure water, the total amount of light absorbed in the seawater column is affected by the combined contribution of particulate matter, both from phytoplankton and non-algal suspended particles, and of coloured dissolved organic matter (CDOM) present in this medium [Bricaud et al. (1998)]. In order to improve the accuracy of existing algorithms for ocean colour remote sensing, and for the development of new ones, it is essential to understand the individual contribution of each of these components in different productivity scenarios [Ferreira et al. (2009)].

Remote sensing of ocean colour has been a particularly useful tool to monitor climate change impacts at a global scale [Brewin et al. (2015)]. Climate change scenarios for the western Iberian Peninsula coast present contradictory forecasts for climate alteration: some predict an enhancement of upwelling events [Bakun (1990), Lorenzo et al. (2005), Ramos et al. (2013), Casabella et al. (2014)], and others predict a decrease in the intensity and the number of upwelling events [Lemos and Pires (2004), Lemos and Sansó (2006), Alvarez et al. (2008), Álvarez-Salgado et al. (2008), Alves and Miranda (2012)]. In an area where fisheries, offshore aquaculture, and marine related tourism are the main economic activities, it is important to develop the most appropriate tools to monitor how climatic change could impact the area. In this context, this study has been conducted to test the overall hypothesis that the determination of the absorption properties of the water column could be used to identify upwelling induced changes in the phytoplankton community. In order to test this hypothesis, this article is structured according to the following research questions:

1) Can bio-optical absorption properties be used to monitor phytoplankton blooms?
2) Are the changes in phytoplankton community and bio-optical parameters of the water column related to the upwelling regimes in the area?

2. Methods

2.1. Study area

The Sagres area is located at the southwest of the Iberian Peninsula (Fig. 1). Seasonal upwelling is induced by northerly winds, mainly occurring from late spring to early autumn [Fiúza et al. (1982), Sousa and Bricaud (1992), Cravo et al. (2010)]. Small upwelling events can also be stimulated by local westerly winds [Relvas and Barton (2002), Loureiro et al. (2008)]. Phytoplankton blooms, especially diatoms, have been reported as a consequence of upwelling events in the area [e.g. Goela et al. (2013)], and dinoflagellate presence has been associated with the relaxation of upwelling conditions [Loureiro et al. (2008)]. The anthropogenic pressures in this coastal area are considered to be low, due to limited agriculture, industry, and population, and no major freshwater inputs [Peliz and Fiúza (1999), Edwards et al. (2005)]. Thus, the contrasting primary productivity scenarios shown in Fig. 1, where TChl*a* concentration attains 5 $\mu g\ l^{-1}$ for bloom conditions (Fig. 1a) and lower than 0.5 $\mu g\ l^{-1}$ for no-bloom conditions (Fig. 1b), can be attributed to differences in upwelling conditions rather than to anthropogenic pressure [Loureiro et al. (2005), Goela et al. (2014)]. The main economic activities in the area are related to the utilisation of coastal resources, dominated by the fisheries industry, although in recent years offshore bivalve aquaculture has assumed an increasingly important role [Edwards et al. (2005)].

2.2. Sampling

Three sampling stations were selected at 2, 10 and 18 Km off the coast of Sagres as validation sites for the MEdium-Resolution Imaging Spectrometer (MERIS), the ocean colour sensor onboard of the ENVISAT European Space Agency (ESA) satellite. A total of 31 sampling campaigns were conducted from autumn 2008 until the spring of 2012 when ENVISAT terminated its mission. They were designed to meet the conditions for MERIS data validation [Doerffer (2002), Barker (2011)], by selecting sampling dates with relatively calm sea and clear sky conditions that matched the ENVISAT overpass (Table 1, Fig. 2).

This paper focuses mainly on the data from the coastal Station A (at approximately 37°00′39″N and 8°53′58″W, see A in Fig. 1) as this

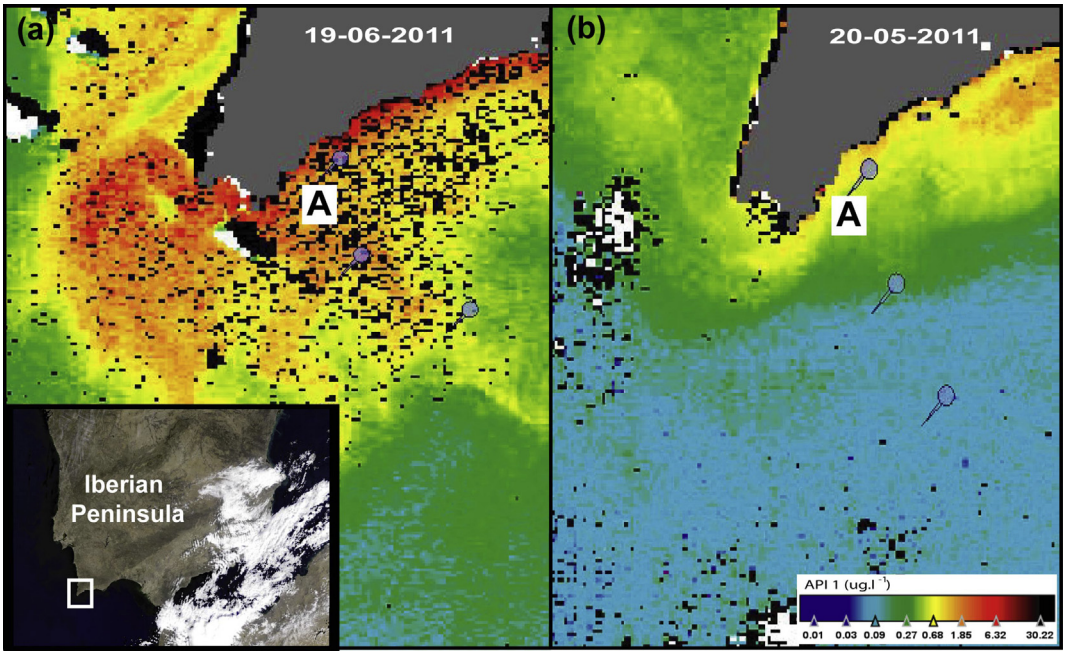

Fig. 1. Ocean colour satellite images (from MERIS) of the study area showing the sampling stations, under (a) bloom (b) and no-bloom conditions. (For interpretation of the references to colour in this figure legend, the reader is referred to the web version of this article.)

Table 1
Examples of sampling dates for bloom and no-bloom conditions, with respective TChl*a* concentrations and total cell abundances in Station A (average and standard deviation from the 3 sampling depths).

Bloom conditions			No-bloom conditions		
Sampling campaign date	[Tchl*a*] (μg l^{-1})	Total abundances (cell ml^{-1})	Sampling campaign date	[Tchl*a*] (μg l^{-1})	Total abundances (cell ml^{-1})
08-11-2008	1.75 ± 0.24	3691 ± 608	17-11-2008	0.67 ± 0.18	970 ± 202
22-04-2009	1.96 ± 0.79	1606 ± 407	14-02-2009	0.45 ± 0.17	529 ± 344
11-07-2009	2.98 ± 0.26	1560 ± 408	21-06-2009	0.54 ± 0.29	1007 ± 345
16-06-2010	2.22 ± 0.40	1630 ± 140	28-05-2010	0.42 ± 0.27	250 ± 105
19-06-2011	2.29 ± 0.32	2254 ± 640	08-07-2010	0.17 ± 0.11	163 ± 124
12-03-2012	6.02 ± 0.30	1960 ± 167	20-05-2011	0.33 ± 0.29	594 ± 53
			14-10-2011	0.48 ± 0.04	291 ± 50
			11-02-2012	0.59 ± 0.02	276 ± 25

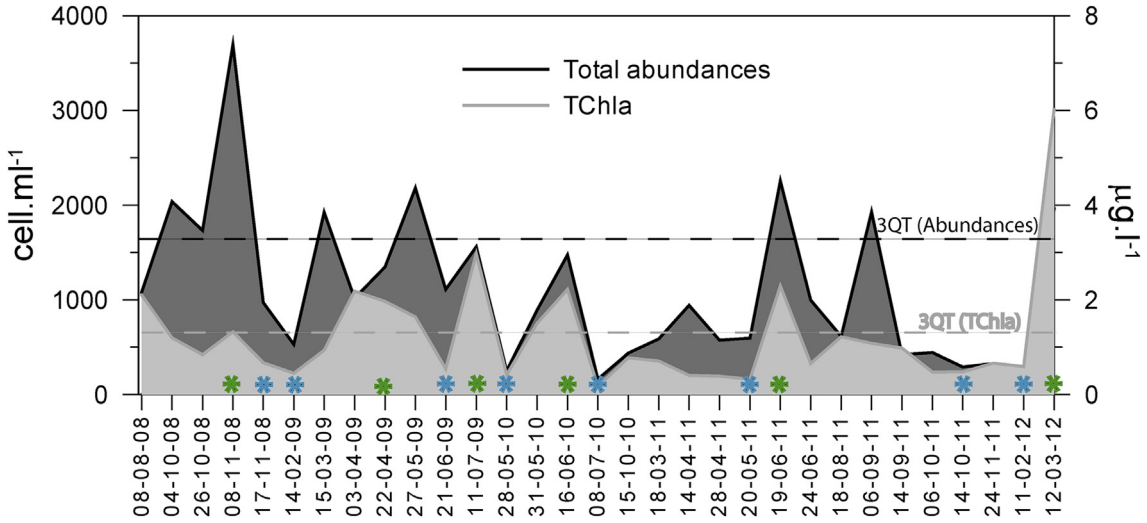

Fig. 2. TChl*a* concentration (μg l^{-1}) and phytoplankton abundances (cell ml^{-1}) represented by dark grey and light grey curves, respectively, for all sampling campaigns at the study site. The dark and light grey horizontal broken lines represent the third quartile for the respective variables (3QT). Selected samples are represented by green asterisks (*) for bloom and blue asterisks (*) for no-bloom conditions.

is the most dynamic site in terms of phytoplankton biomass, probably due to its proximity to the coastline, where blooms are more evident and frequent and, thereby, producing a much more robust dataset for bloom events compared to normal conditions. The more offshore Stations were also taken into account (see blue points in Fig. 1) to evaluate the influence of coastal inputs to the TChl*a* concentration. Sampling at the Stations is Langrangian, which means that the specific location in terms of latitude and longitude will vary for each sampling campaign, depending on the weather and sea conditions (note the slight differences in the Station locations between Fig. 1a and b).

Temperature profiles were acquired from a CTD (SBE® 19 plus SeaCAT). A Niskin bottle was used to collect water samples, which were then kept protected from light, in 10 l Nalgene® (for phytoplankton pigment determination) and 0.5 l glass containers (for CDOM determination).The sampling period for all three Stations was within 2–3 h, and all samples were processed within a period of 3 h after arrival onshore. Although water was collected at 3 different depths (surface, mid-Secchi and Secchi depths), data on the phytoplankton pigments as well as bio-optical parameters were averaged for the three depths of the water column, as generally the water column within the Secchi depth is well mixed [Goela et al. (2013)].

At the field laboratory, 2–3 l of water were filtered through Whatman® 47 mm GF/F filters, and preserved in liquid nitrogen for pigment analysis. For particulate absorption measurements, duplicates of 0.5 l were filtered through Whatman® 25 mm GF/F filters, stored in tissue capsules and also kept in liquid nitrogen. Regarding the CDOM absorption, 0.2 l of the samples from each glass bottle was filtered through Whatman® 47 mm polycarbonate membrane filters; the filtrate was then kept in glass dark bottles at −4 °C, until further analysis (within 24 h). For phytoplankton analysis, samples were preserved in Lugol iodine, after being passed through a 200 μm mesh, to remove the larger organisms.

2.3. Phytoplankton community

The phytoplankton pigments were quantified by HPLC, following Wright and Jeffrey (1997) methodology. The samples from 2008 until July 2009 were determined in a Waters® 600E HPLC system, equipped with Diode Array Detection (DAD), and using a C18 Thermo® Hypersil-Keystone (ODS-2) column (25 cm of length, 4 mm of diameter and 5 μm of particle size). All the other samples were determined with an Agilent® 1200 with DAD equipment, using a C18 Alltech® Altima column (15 cm of length, 4.6 nm of diameter and 3 μm of particle size). The extraction procedures included the soaking of the sample filters in acetone during 4 h, followed by sonication (20 s) to improve extraction efficiency. Each extract was centrifuged and the clear supernatant was injected into the HPLC-DAD system. The chosen wavelengths of detection for chlorophylls and carotenoids were 436 nm and 450 nm, respectively. The phytoplankton community was also observed by inverted microscopy technique, following the Utermöhl (1931) method modified by Evans (1972) and using a Zeiss Axiovert 15 inverted microscope. For further details on these methodologies please see Goela et al. (2013).

With the results from the HPLC technique, it was possible to run the CHEMTAX v. 1.95 software [Mackey et al. (1996)], to obtain the contributions of each individual phytoplankton class to TChl*a*. The classes uploaded to the configuration of CHEMTAX were chrysophytes, cryptophytes, cyanobacteria, diatoms, dinoflagellates, prasinophytes, and prymnesiophytes. The classes were chosen based on the pigment markers – peridinin, 19'hexanoyloxifucoxanthin, fucoxanthin, 19'butanoyloxifucoxanthin, violaxanthin, alloxanthin, lutein, zeaxanthin, Chlorophyll *b* and Chlorophyll *c3* – found in the samples, and from the previous literature on the local phytoplankton community [Loureiro et al. (2005), Loureiro et al. (2008), Goela et al. (2013)]. Chlorophytes were excluded from these analysis as the pigment markers shared with prasinophytes (Chlorophyll *b*, neoxanthin, violaxanthin and β-caroten) are highly correlated with prasinoxanthin, which is an exclusive pigment from prasinophytes, as detailed by Mendes et al. (2011) and Goela et al. (2014) (please see Goela et al. (2014), sections 2.4 and 3.2, for data on correlations and a more detailed explanation). Initial pigment to TChl*a* ratios were obtained from the literature [Schlüter et al. (2000), Gibb et al. (2001)], and are presented in Table 2, together with the final ratios obtained with CHEMTAX software.

The long-term variability of the TChl*a* concentration was assessed with the analysis of a time series for MERIS Algal Pigment Index 1 (API 1, i.e. MERIS ocean colour product, equivalent to TChl*a* concentration) obtained during the coverage of ENVISAT, between 2002 and 2012. API 1 data was extracted from MERIS Level 2 Reduced Resolution satellite images, with a spatial resolution of 1.2 km × 1.04 km, using Basic ERS & ENVISAT (A) ATSR and MERIS toolbox (BEAM version 4.9) software. More detailed explanations of the data extraction procedures are in Cristina et al. (2014, 2015).

2.4. Bio-optical parameters

The coefficients of absorbance for total particulate matter (a_p) were determined with the "Transmittance-Reflectance" technique [Tassan and Ferrari (1995), (2002)], using a dual-beam spectrophotometer (GBC CINTRA 40), equipped with an integrating sphere, which has the advantage of eliminating errors from backscattering of light by the particles, which is not possible with the conventional light-transmission technique [Yentsch (1968)]. With the Transmittance-Reflectance procedure, the absorption by the particles due to a normally incident unitary parallel light beam on a single through-way (a_s) can be described by equation (1):

$$a_s = \frac{1 - pT + R_f(pT - pR)}{1 + R_f pT\tau} \quad (1)$$

In this equation, pT and pR are the ratios resultant from the measurements in the transmission and reflectance modes, respectively; the filter reflectance, R_f, is obtained from a measurement in the reflection mode; the factor τ is determined from equation (7) in Tassan and Ferrari (1995, 2002) and it accounts for the diffuse nature of the backscattered radiation. More detailed information on these ratios and variables may be obtained from the original papers [Tassan and Ferrari (1995, 2002)]. The optical density can be determined by equation (2):

$$A_s = \log\left(\frac{1}{1 - a_s}\right) \quad (2)$$

and converted into the equivalent optical density of the particle suspension (correction for path length amplification factor), by the means of the empirical correlation $A_{sus}(\lambda) = 0.423\, A_s(\lambda) + 0.479\, A^2(\lambda)$. Given the ratio between the filter clearance area and the volume of filtered sample (X), the coefficient of particulate absorption (a_p) can be determined by equation (3):

$$a_p(\lambda) = 2.3 A_{sus}/X \quad (3)$$

The fraction of light absorbed by the phytoplankton, expressed through its coefficient, a_{ph}, was discriminated from the light absorbed by non-algal particles, a_{nap}, through the bleaching of the filters with 10% active sodium hypochlorite [Ferrari and Tassan (1999)]; a_{ph} was then determined by subtracting the non-algal

Table 2
Initial and output pigment: Chl*a* matrices applied in CHEMTAX analysis of pigment data.

Class/pigment	Per	19'But-fuco	Fuco	19'Hex-fuco	Viola	Allo	Lut	Zea	Chl *b*	Chl *c3*
Initial										
Prasinophytes	0	0	0	0	0.14	0	0.018	0.079	0.68	0
Dinoflagellates	1.06	0	0	0	0	0	0	0	0	0
Cryptophytes	0	0	0	0	0	0.23	0	0	0	0
Cyanobacteria	0	0	0	0	0	0	0	0.59	0	0
Diatoms	0	0	0.76	0	0	0	0	0	0	0
Crysophytes	0	1.56	0.97	0	0	0	0	0	0	0.25
Prymnesiophytes	0	0.020	1.21	1.36	0	0	0	0	0	0.17
Output										
Prasinophytes	0	0	0	0	0.14	0	0.019	0.084	0.85	0
Dinoflagellates	1.17	0	0	0	0	0	0	0	0	0
Cryptophytes	0	0	0	0	0	0.11	0	0	0	0
Cyanobacteria	0	0	0	0	0	0	0	0.62	0	0
Diatoms	0	0	2.03	0	0	0	0	0	0	0
Crysophytes	0	1.46	1.07	0	0	0	0	0	0	0.27
Prymnesiophytes	0	0.016	1.02	1.41	0	0	0	0	0	0.20

absorption spectra (bleached filter) from the total particulate spectra (before bleaching), a_p. To derive the phytoplankton specific coefficient of absorption (a^*_{ph}), each spectrum of a_{ph} was normalised by the respective TChl*a* concentration. For further details on the determination of coefficients of particulate matter please see Goela et al. (2013), Tassan and Ferrari (1995, 2002).

The standard method for the determination of the coefficient of absorbance of CDOM, a_{CDOM}, developed for the validation of MERIS Chlorophyll products in North Sea coastal waters [Tilstone et al. (2002)], was used in this study. This protocol is based on the approaches of Mitchell et al. (2000), Mueller and Austin (1995) and Pegau and Zaneveld (1993). A GBC CINTRA 40 spectrophotometer was used, with a 10 cm path length glass cylindrical cell. Reference spectra were obtained with filtered (polycarbonate membrane, 0.2 μm porosity filters) Lichrosolv® water, and recorded immediately prior to the sample readings.

2.5. Upwelling indices and sea surface temperature data

To study the influence of upwelling on the phytoplankton community and changes in bio-optical properties, upwelling conditions were quantitatively described based on upwelling indices derived from wind stress and sea surface temperature (SST). Ekman transport was calculated from the wind stress following Bakun (1973) and Cropper et al. (2014). The latitudinal (Q_x) and longitudinal (Q_y) components were considered to be the upwelling indices for the Western (Q_x) and Southern (Q_y) coasts, given that coastline directions in the study area can be described as roughly parallel to the meridian (West coast) and the equator (South coast). Therefore, negative values of Q_x and Q_y indicated upwelling conditions along the Western and Southern coasts in the study area, respectively. Wind speed and direction data were obtained from the Blended Daily Averaged 0.25-degree Sea Surface Winds (at 10 m level) product, provided by the National Oceanic and Atmospheric Administration (NOAA) and National Climatic Data Center [Zhang et al. (2006)].

SST data used were extracted from the NOAA Optimum Interpolation (OI) daily SST at 0.25-degree resolution model [Reynolds et al. (2007)] (SST^{OI}). The SST based upwelling index, UI^{SST}, was calculated as the difference in SST values between sampling Station A (N 37.0° W 8.9°), representing coastal conditions and a location at 1° to the West at the same latitude (N 37.0° W 9.9°), representing oceanic conditions. Positive values indicated lower SST at the coastal Station and therefore increase in upwelling intensity. The daily SST anomaly was calculated as a difference between SST on each day of the year and the average SST for that day over the period from 10th July 1987 to 31st December 2013.

All wind and SST data were accessed via the NOAA Environmental Research Division Data Access Program (ERDDAP) at http://upwell.pfeg.noaa.gov/erddap/index.html (last accessed on 04/09/2014).

2.6. Bloom versus no-bloom conditions: criteria

The definition of phytoplankton or algal bloom is known to be relative, often relying on subjective criteria such as growth rate, biomass, or both [Kutser (2009), Blondeau-Patissier et al. (2014)]. Thus, it is important to define this terminology in the frame of this study before going any further. The quantitative criteria to select bloom events are based on discrete samples with both a high TChl*a* concentration and a high abundance of cells. To define "high" concentration of these two metrics, the main statistical descriptors such as the average and third quartile were determined for the two variables. The bloom condition criteria were defined as follows: TChl*a* concentration and total abundances exceeding the third quartile, or where one of these metrics was 25% above the third quartile, and the other was above the average.

This concept can be better understood by looking at the concentrations of TChl*a* and total cell abundances graphs shown in Fig. 2. Examples of sampling dates considered for both bloom and no-bloom conditions are shown in Table 1. In order to ensure a balanced comparison between bloom and no-bloom conditions, a total of 12 sampling campaigns were chosen from those for each condition: 6 in bloom and 6 in no-bloom. Whenever possible, each no-bloom sampling campaign was selected closest to a date for a bloom sampling campaign, to serve as a reference value before or after the bloom event. Although some other dates could also be considered as bloom events during the sampling period, on the basis of the criteria presented above (e.g. 27th May 2009), these were not considered due to the lack of a complete bio-optical dataset.

2.7. Data treatment and statistical analysis

The statistical analysis was performed with the Statistica® 10 (Stat. Soft Inc.) package. Whenever needed, the non-parametric Spearman correlation analysis was used to evaluate the degree of correlation between the study variables. Analysis of Variance (ANOVA), followed by Fisher's Least Significant Difference (LSD) tests were carried out using "bloom" and "no-bloom" conditions as the categorical predictors. The level of significance for the statistical analysis was $\alpha = 5\%$; thus, the result was considered significant

whenever the *p*-value (p) was $<\alpha$. The API 1 time series of monthly mean data was decomposed into seasonal, trend and residuals components by the classical decomposition method, using R software [R Core Team (2015)]. Both additive and multiplicative models were fitted to the data, and the multiplicative model was chosen on the basis of a lower root mean square error (RMSE).

3. Results

3.1. Phytoplankton community

During the period of study, significant changes were observed in the group dominance of phytoplankton community during bloom events, compared to no-bloom events (Fig. 3). On the basis of the CHEMTAX results, the diatom contribution to TChl*a* during bloom conditions is significantly higher (average of 63%) than the joint contribution of the other classes. From the six sampling campaigns coinciding with bloom periods, the microscopic identification of diatoms revealed the presence of *Chaetoceros* spp. in significant numbers in all of the samples, but also the presence of *Leptocylindrus* (22nd April 2009 and 19th June 2011), *Pseudo-nitzschia spp.* (11th July 2009) and *Guinardia delicatula* and *G. striata* (12th March 2012) in significant abundance. Potentially harmful species detected during this study include the toxic dinoflagellates *Dinophysis acuminata*, *D. ovum*, *D. caudata*, *Lingulodinium polyedrum*, *Prorocentrum micans*, *Gymnodinium catenatum* and *Scrippsiella trochoidea*. Diatoms of the genus *Pseudo-nitzschia* were not identified to species level, but nonetheless belong to a genus that includes toxic species.

Considering the periods with low phytoplankton abundance associated with low concentrations of TChl*a*, the joint contributions of prasinophytes, chryptophytes and prymnesiophytes and sometimes cyanobacteria to TChl*a* made up more than 50% of the TChl*a* concentration, with an average of 71% (Fig. 3b). The microscope counts also reflected these results, with an average of 63% of the phytoplankton cells counted falling into the unidentified small flagellate group, which is clearly dominant in the majority of the sampling dates considered to be no-bloom (Fig. 3b, d). In these periods, the diatoms contribution to TChl*a* was on average 24%. Dinoflagellates were not a dominant group during either bloom or in no-bloom conditions and, on the basis of microscope counts, represented only 3% and 8% of the total community, respectively.

The long-term variability of the TChl*a* concentration of the study is shown in Fig. 4a. The API 1 binned per month (Fig. 4b) showed that the TChl*a* means (10 years of data) were higher in spring and summer months. In agreement with the study of Cloern and Jassby (2010), the standard deviation of the standardised components (Fig. 4 c, d, and e) showed that the residual and seasonal components are contributing most to the variability of TChl*a* at Sagres.

The *in situ* parameters water temperature, together with upwelling indices, were chosen in this study to evaluate upwelling events in the area and its relation with the observed bloom conditions. Considering the whole period of study, there were significant negative correlations between the main proxy for phytoplankton biomass, TChl*a*, and the variables temperature (*in situ*) and distance from coast ($r_s = -0.44$, $p < 0.05$, between temperature and TChl*a* and $r_s = -0.29$, $p < 0.05$ between TChl*a* and distance from coast). Also, to illustrate oceanographic forcing of the bloom events, the upwelling indices Q_x, Q_y, SST^{OI}, SST anomaly, and UI^{SST} were plotted and analysed together (Fig. 5). The annual-scale

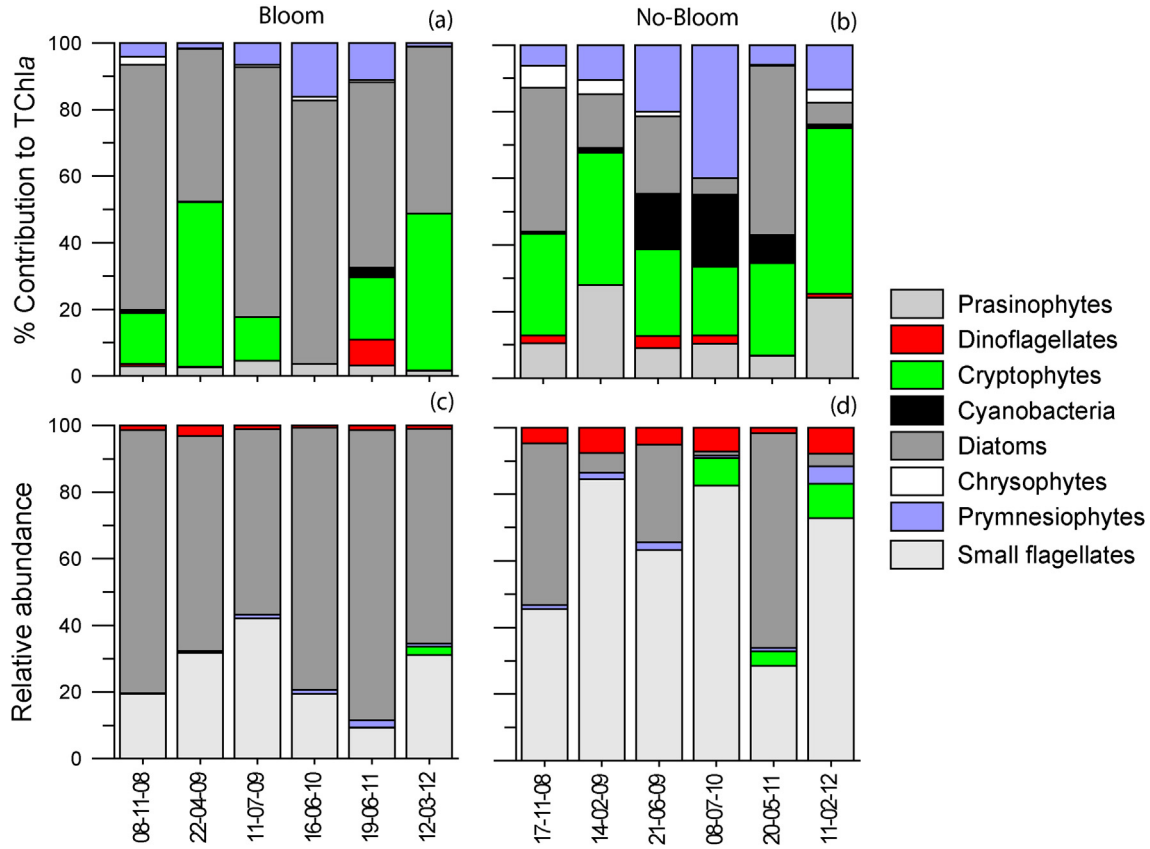

Fig. 3. Phytoplankton community as represented by CHEMTAX (upper panel) and inverted microscopy (lower panel) techniques, in bloom (a and c) and in no-bloom (b and d) conditions. Please note that only the relative abundance of coccolitophorids are represented by "prymnesiophytes" (c and d).

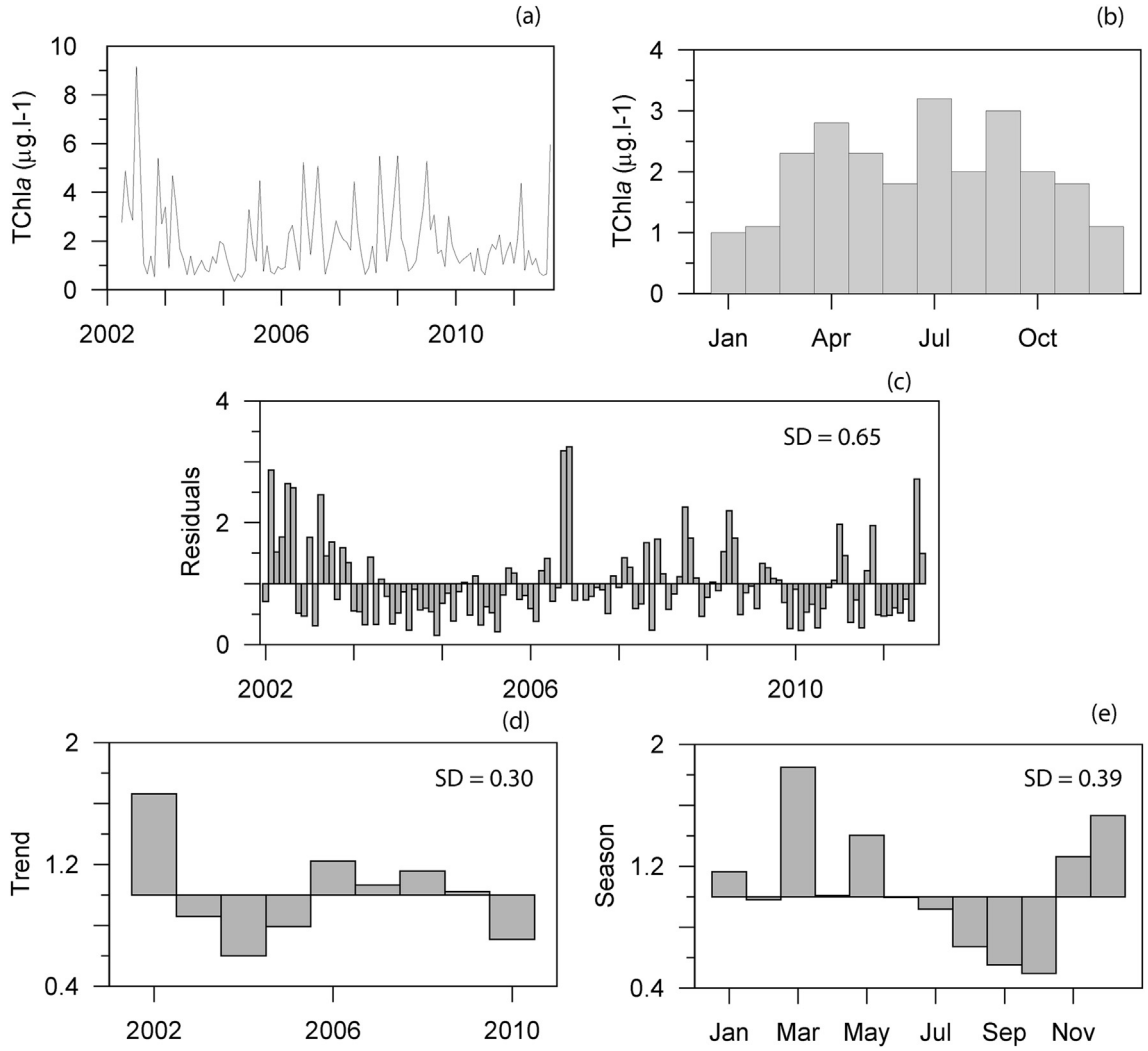

Fig. 4. TChl*a* obtained from the MERIS sensor over the operational life of ENVISAT (2002–2012): (a) on a normal time scale; (b) binned per month; (c) standardised decomposed residual; (d) standardised decomposed trend; and (e) standardised decomposed season. Components for the time series are based on the approach of Cloern and Jassby (2010).

variation of wind based upwelling index (Fig. 5a) showed that upwelling in the study area was more active during summer (May–September) and connected with Northerly and N-Westerly winds with shorter upwelling events during the winter season. From the examination of plots in Fig. 5(b–g), it was evident that sampling dates with bloom conditions were characterised by:

1) Negative SST difference (anomaly) typically in the range of 0.25–1.5° lower than the 26-year average for the corresponding day of the year;
2) Upwelling favourable values of Ekman transport at Western and/or Southern coast;
3) Lower SST near the coast compared to oceanic conditions 1° to the West offshore.

The conditions described in some cases persisted for longer than 3–4 weeks (22nd April 2009, 16th June 2010 and 19th June 2011), or occurred 7–10 days before the sample dates. In other cases, the maximum values had already decreased at the time of sampling (12th March 2012). Nonetheless, their effects on the phytoplankton community, productivity and optical properties were still observable.

3.2. Bio-optical parameters

The particulate absorption coefficients, a_p and a_{ph}, were analyzed at 443 and 678 nm, wavelengths that represent the maxima of absorbance of chlorophyll *a*. In the blue region of the spectrum, the mean values of a_p and a_{ph} were significantly higher in bloom conditions (0.10 ± 0.03 m^{-1} and 0.09 ± 0.03 m^{-1}, respectively) than in no-bloom conditions (0.045 ± 0.015 m^{-1} and 0.037 ± 0.012 m^{-1}, respectively) (Wilk's test, $F = 6.7$, $p < 0.05$). Regarding the red part of the spectrum, the same pattern was observed with mean values of a_p and a_{ph} being elevated by a factor between of 2 and 3 between bloom to no-bloom conditions ($a_p = 0.053 \pm 0.017$ m^{-1} and $a_{ph} = 0.053 \pm 0.016$ m^{-1}, during bloom conditions and $a_p = 0.019 \pm 0.009$ m^{-1} and $a_{ph} = 0.016 \pm 0.007$ m^{-1}, in no-bloom conditions). Fig. 6 shows the marked difference in the phytoplankton absorption between the two contrasting productivity conditions in the study area. Besides the magnitude of the a_{ph} spectra in both maximums of absorbance, the ratio between the two maxima of absorbance (blue:red) was also analyzed to evaluate possible changes in the shape of the spectrum between the two contrasting conditions. The results showed that during bloom conditions the blue:red ratio was significantly lower than during no-bloom conditions (blue:red $= 1.83 \pm 0.12$ for bloom and blue:red $= 2.37 \pm 0.27$ for no-bloom) (Wilk's test, $F = 19.6$, $p < 0.05$)

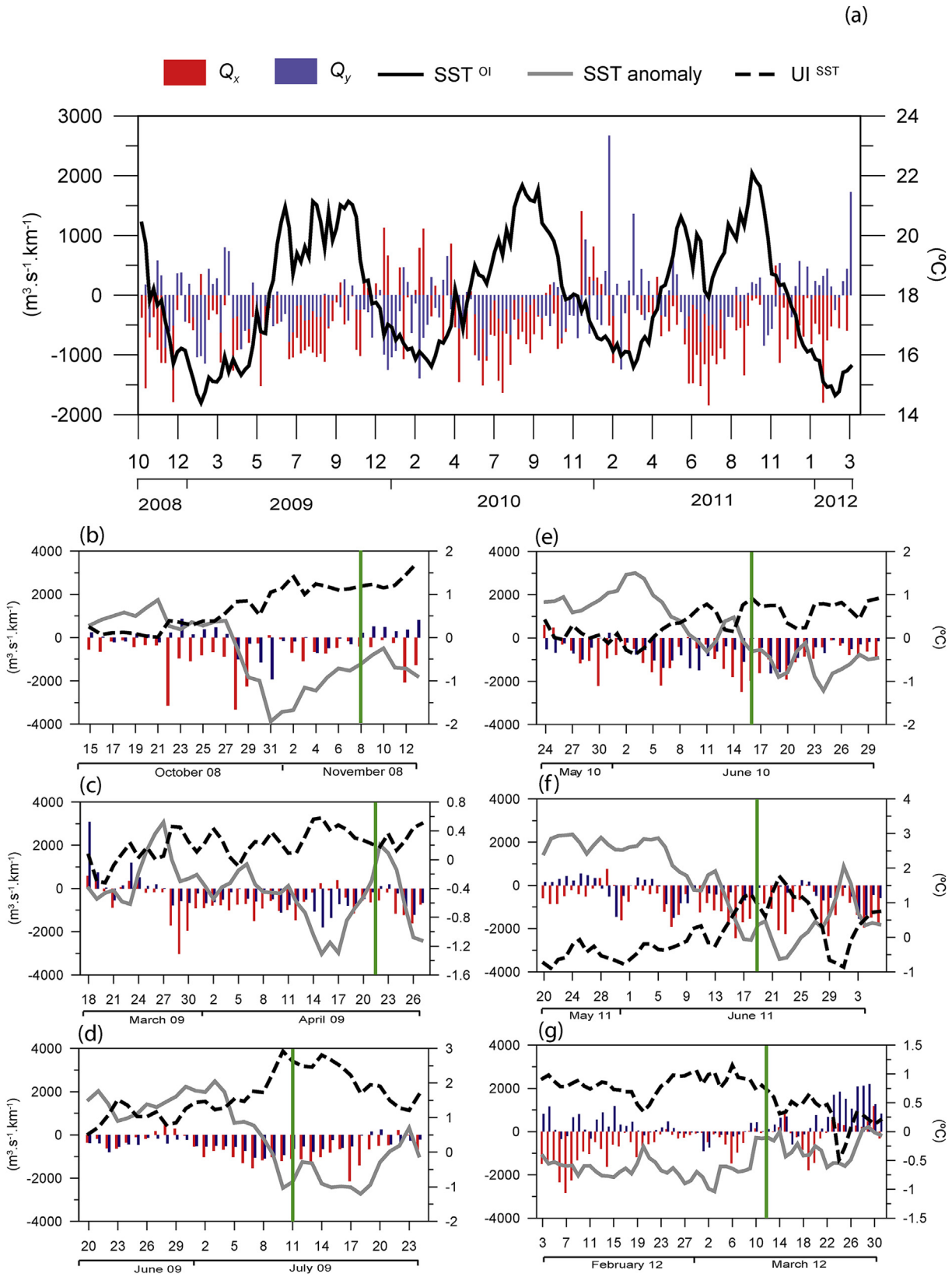

Fig. 5. (a) Temporal variability of weekly averaged Ekman transport components along the Western (Q_x) and Southern (Q_y) coast together with weekly averaged sea surface temperature (SST^{OI}) over the duration of the study (Oct 2008–March 2012); (b–g) wind stress based upwelling indices (Q_x and Q_y) and SST based upwelling indices (UI^{SST}) from a daily perspective, with time windows over 1–2 months in the vicinity of each bloom event (marked as green lines in each of the figures), together with daily SST temperature anomalies (SST anomaly). Negative values of Q_x and Q_y and positive values of UI^{SST} indicate conditions favourable for upwelling. (For interpretation of the references to colour in this figure legend, the reader is referred to the web version of this article.)

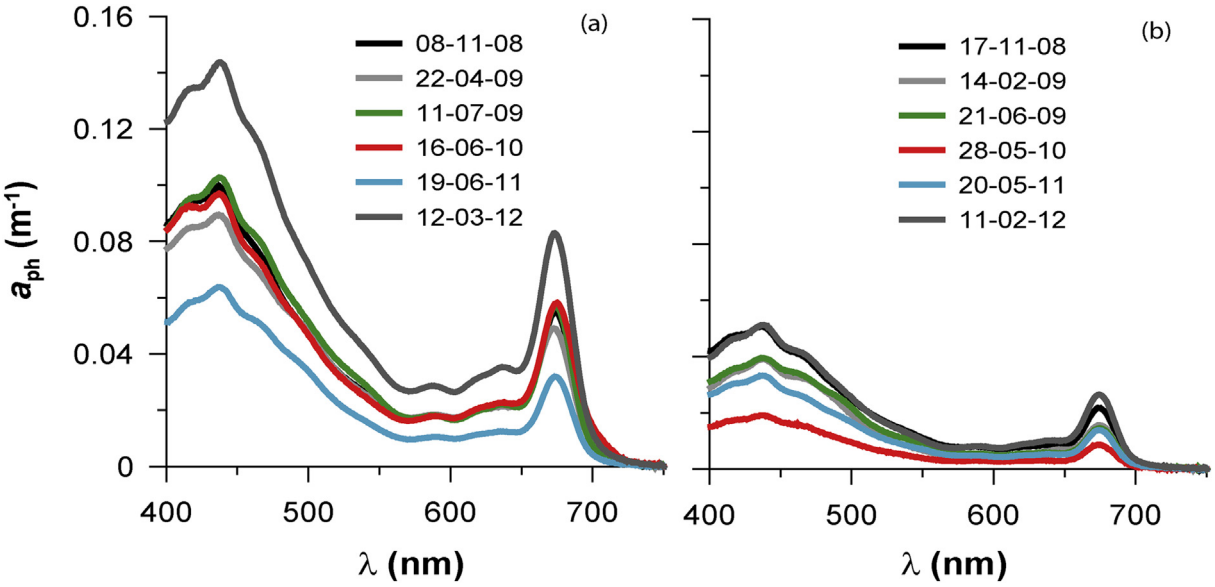

Fig. 6. Spectra of phytoplankton coefficient of absorption under a) bloom and b) no-bloom.

(Fig. 7).

Similarly to what happens with TChl*a*, both $a_{ph}(443)$ and $a_{ph}(678)$ presented significant negative correlations with water temperature ($r_s = -0.27$ and $r_s = -0.36$, $p < 0.05$ respectively). Regarding the blue:red ratio, there was a positive correlation with the same parameter ($r_s = 0.66$, $p < 0.05$).

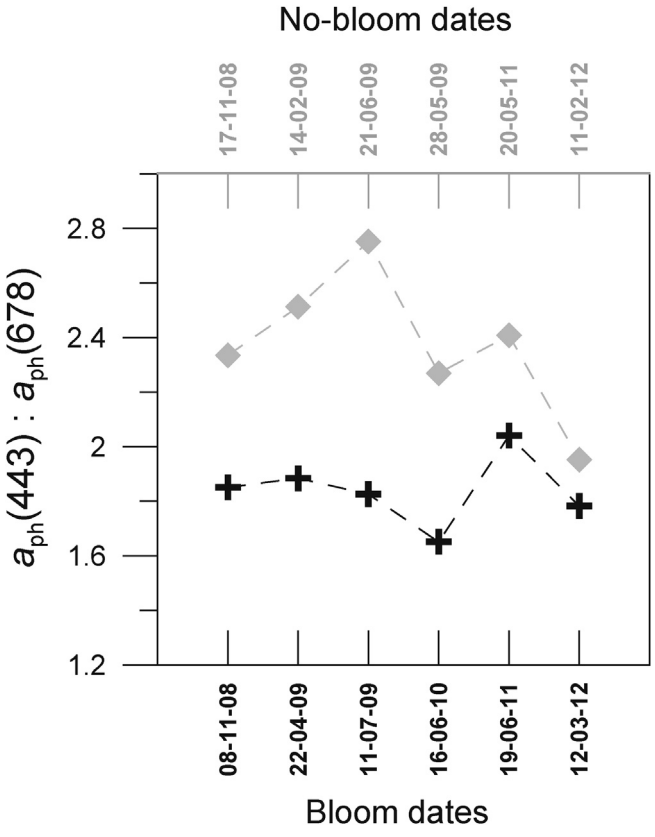

Fig. 7. Blue:red ratios of a_{ph} in bloom (black crosses with dates on lower *xx* axis) and no-bloom (grey diamonds with dates on upper *xx* axis) conditions.

The specific phytoplankton absorption coefficient (a^*_{ph}) presented statistically lower values during bloom conditions at 443 nm (0.040 ± 0.018 m^2 mg^{-1}) when compared to no-bloom conditions (0.075 ± 0.018 m^2 mg^{-1}) (Wilk's test, F = 11,99, $p < 0.05$). At 678 nm, a^*_{ph} presented a marginally significant difference ($p < 0.1$) between bloom and no-bloom conditions: a^*_{ph} during bloom state (mean of 0.022 ± 0.009 m^2 mg^{-1}) had lower values compared to the no-bloom conditions (mean of 0.032 ± 0.009 m^2 mg^{-1}).

The coefficient of absorption by non-algal particles, a_{nap}, at 443 nm presented no significant differences between bloom and no-bloom conditions.

In the dissolved fraction of the absorption spectra, the mean of $a_{CDOM}(443)$ in bloom conditions was lower (0.050 ± 0.009 m^{-1}) than in no-bloom conditions (0.068 ± 0.015 m^{-1}) (Fig. 8 a,b), although the difference is not statistically different. Similarly, no significant differences were observed in the slopes of the a_{CDOM} between bloom (-0.010 ± 0.003 m^{-1}) and no-bloom conditions (-0.011 ± 0.006 m^{-1}).

4. Discussion

The usefulness of the bio-optical data from the water column as a tool to detect phytoplankton blooms can only be demonstrated if the inherent optical properties show significant differences between conditions of high and low phytoplankton biomass. By grouping the bio-optical data into “bloom” and “no-bloom” conditions, it has been possible to observe differences between these two conditions.

In the study area, a_{ph} changed markedly between the two situations, increasing by a factor of 2–3 in bloom conditions at both wavelengths maximums of 443 and 678 nm. Taking into account that the mean concentration in the bloom period is 2.8 μg l^{-1} and in the no-bloom is 0.50 μg l^{-1}, these *in situ* results are in agreement with the models presented in Goela et al. (2013) for comparing TChl*a* concentration with $a_{ph}(443)$ and $a_{ph}(678)$ (see Fig. 6 in Goela et al., 2013). These models predicted values of 0.089 m^{-1} and 0.041 m^{-1} for $a_{ph}(443)$ and $a_{ph}(678)$, respectively, at a concentration of 2.8 μg l^{-1} for TChl*a*, and values of 0.034 m^{-1} and 0.013 m^{-1} for the same coefficients, at a concentration of 0.5 μg l^{-1} for TChl*a*. These values from the models are similar to the *in situ* values from

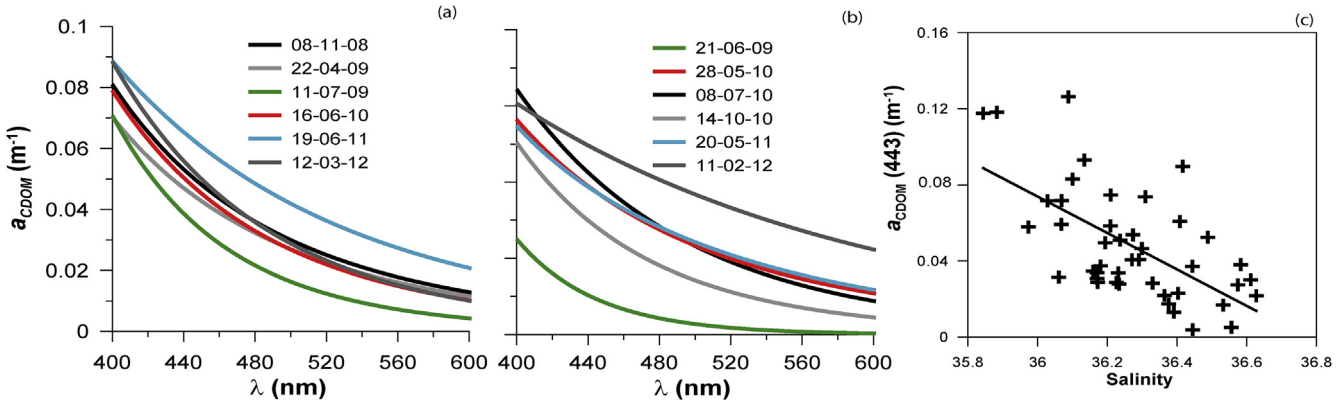

Fig. 8. Spectra for the coefficient of absorbance of CDOM under (a) bloom and (b) no-bloom conditions. (c) Relationship between $a_{CDOM}(443)$ and salinity at Station A.

this study, with averages of 0.096 m^{-1} and 0.037 m^{-1} for $a_{ph}(443)$ and $a_{ph}(678)$, respectively, at a concentration of 2.8 μg l^{-1} concentration for TChl*a*, and values of 0.037 m^{-1} and 0.016 m^{-1} for the same coefficients, at a concentration of 0.5 μg l^{-1} for TChl*a*. Besides these differences in the values for a_{ph}, there are changes in the shapes of the coefficient spectra, with increasing blue:red ratios in no-bloom conditions. Higher blue:red ratios have been attributed to the dominance of a system by phytoplankton populations with small cell sizes [Millán-Nuñez et al. (2004)].

As might be expected [Bricaud and Stramski (1990)], the mean values of $a^*_{ph}(443)$ decreased markedly between bloom and no-bloom conditions at Sagres. According to Babin et al. (1993), this bio-optical parameter could vary up to 4 times in value at this wavelength as a result of changes in the intracellular pigment concentration and cell diameter of the phytoplankton community. Babin et al. (1993) also comment on the influence of cell size on the "package effect" (decreased efficiency of light absorption due to the fact that the pigments are packaged within the cell and not in solution). According to these authors, the decrease in the $a^*_{ph}(443)$ values observed in this study (0.075 m^2 mg^{-1} to 0.040 m^2 mg^{-1}) is consistent with a change in the cell size of the phytoplankton community; this change could comprise an increase from cells of 1 μm (mean cell diameter) and 1–2 kg m^{-3} of intracellular pigment concentration to cells of 3–5 μm (mean cell diameter) and 4–8 kg m^{-3} of intracellular pigment concentration (see Fig. 6 in Babin et al. (1993)). Other studies have also reported that changes in phytoplankton size distribution and pigment composition are the main factors influencing $a^*_{ph}(443)$ [Yentsch and Phinney (1989), Ciotti et al. (1999), Bricaud et al. (1995, 2004)]. At Sagres, the flattening of a^*_{ph} spectrum is considered to be caused primarily by changes in the size structure of the phytoplankton community, with a small, but relevant contribution from pigment composition [Goela et al. (2013)]. Indeed, the major contributors to TChl*a* concentrations under bloom conditions are diatoms, whilst under no-bloom conditions they are small-sized phytoplankton classes (Fig. 3).

Regarding $a^*_{ph}(678)$, there are no major differences between bloom and no-bloom conditions; this is would be expected because of the lower impact of the "packaging effect" and the contribution of accessory pigments in this area of the spectrum [Babin et al. (1993)]. However, this parameter could decrease slightly in bloom conditions, taking into account the statistically significant differences found for a lower level of confidence (10%). This is an important parameter in radiative transfer models; therefore this change may be important when considering the development and adjustments to regional algorithms for remote sensing ocean colour.

The absorption of light by non algal particles (a_{nap}) at the Sagres site shows no significant differences between bloom and no-bloom conditions. Indeed, Cristina et al. (2014) also found that this parameter was constant both over the temporal period of study, and along the spatial gradient from inshore to offshore. Given that sediment dynamics near to the coast are generally under human influence (e.g. presence of dams, irrigation works or dredging), it is evident that the anthropogenic pressure at Sagres is minimal.

The dissolved fraction of absorbance has also been determined in this study. Remote sensing of ocean colour relies mostly on water leaving reflectance, which is strongly related to the sum of the phytoplankton absorption (a_{ph}) and the CDOM absorption (a_{CDOM}) [Lyon et al. (2004)]. The $a_{CDOM}(443)$ parameter does not present significant differences between bloom and no-bloom condition, and no relationship has been observed between $a_{CDOM}(443)$ and TChl*a*, which suggests that the origin of the CDOM is not probably from the phytoplankton-derived components, as is typical for oceanic environments [Bricaud et al. (2010)]. To evaluate the influence of the terrestrial inputs on the a_{CDOM}, the $a_{CDOM}(443)$ has been plotted against salinity (Fig. 8c) in the study area. A significant inverse relationship is found ($r_s = -0.58$, $p < 0.05$), meaning that the CDOM origin is more likely to be from the freshwater inputs from the coast in Sagres; similar results have been observed in other coastal areas (e.g. [Vantrepotte et al. (2007)]). Finally, the absorption of a_{CDOM} relative to the total absorption of $a_{CDOM} + a_p$, constitutes 33–60% (bloom and no-bloom, respectively), at 443 nm. Given that no co-variation has been observed with TChl*a*, this suggest a possible classification for Case 2 type water, as $a_{CDOM}(443)$ could interfere with the retrieval of TChl*a* by remote sensing and, for this reason, should not be neglected [Sathyendranath (2000), Smith et al. (2013)], especially, under conditions of low productivity. Cristina et al. (2009, 2014, 2015) demonstrated that, despite the good agreement between MERIS API 1 and *in situ* data, this agreement decreases with the proximity to the coast. Although much of this discrepancy could be attributed to adjacency effects, the influence of dissolved components of absorbance could also be causing some degree of bias. The neural net MERIS API 2 product (equivalent to TChl*a* concentration in Case 2 type waters) has been developed to deal with these interferences [Doerffer and Schiller (2007)]. However, some studies suggest that neural network processors perform worse in waters dominated by CDOM absorption and with low concentrations of pigments [Doerffer and Schiller (2007), Beltrán-Abaunza et al. (2014)]; this can cause an overestimation of pigment concentration at low values, even when API 2 is used [Beltrán-Abaunza et al. (2014)].

These differences in absorption between bloom conditions and no-bloom conditions strongly suggest that bio-optical parameters

can be used to assess shifts in the phytoplankton community. Furthermore, it makes sense to explore if this outcome could be somehow related with upwelling regimes in the area.

As this is a coastal region, it would be expected that anthropogenic inputs on the primary productivity would be significant. However, the results show that the phytoplankton biomass is more strongly (negatively) correlated with temperature than with the proximity to the coast. Furthermore, the phytoplankton absorption properties also present significant relationships with temperature, both in magnitude of the phytoplankton absorption coefficients at the blue and red maxima, and with the shape of the phytoplankton spectra (blue:red ratio). Although in some regions of the globe, diatoms blooms are stimulated by windier conditions and elevated concentrations of nutrients occurring during winter runoff [Margalef (1978)], at Sagres, diatom blooms are mostly associated with spring and summer [Goela et al., 2014] (Fig. 4a), when upwelling events are more frequent. Indeed, after the residual component (Fig. 4c), the seasonal component (Fig. 4e) of the long API 1 time series explains a significant amount of the variability in the TChl*a* concentration in the region. According to Cloern and Jassby (2010), this observation is typical for phytoplankton patterns in coastal regions around the globe. The processes causing high variability in the residuals component are, for example, the presence of sampling irregularities (e.g. data gaps, random errors), or the occurrence of singular events of exceptionally high biomass; whilst the strong seasonal component is present where the governing processes are linked to an annual climate cycle, with a good example provided by the seasonal upwelling regime in Sagres (Fig. 5a).

In this study, negative temperature anomalies, associated with favourable wind conditions (upwelling indices), are observed a few days before the bloom sampling dates. However, these temperature differences observed with the mean multiannual values (SST anomaly) could not be attributed solely to seasonality. A comparison of SST with an oceanic site away from the coastal influence at the same latitude identifies the existence of water masses with low temperatures near coast, which strongly suggests that cold, nutrient-rich, upwelled water in the area has a greater influence on the phytoplankton dynamics than the influence from anthropogenic activities in the vicinity. These findings corroborate the findings of Loureiro et al. (2005), who concluded that in the Sagres area, the physical parameters were the primary factors influencing the microplankton structure and distribution. Although a more focused and objective study on the persistence of blooms after favourable upwelling conditions, including collection of regular samples for phytoplankton community analysis before and after the bloom, would be necessary to fully understand the persistence of blooms after favourable upwelling conditions diminish. Previous studies in the area have demonstrated that the diatom bloom collapses were not only due to relaxation of upwelling conditions [Loureiro et al. (2005)], but were also closely connected with silicate limitation [Goela et al. (2014)].

In this context, it might be logical to think that the increase in the number of upwelling events in the area would also increase the biomass production, which would benefit the fisheries and aquaculture industries. On the other hand, may be the increased phytoplankton blooms will also potentially lead to the increase of HAB toxins, which could impact negatively the same industries. However, several other studies in the Iberian coast report that the harmful species are most likely to bloom during periods of upwelling relaxation [Palma et al. (1998), Reguera et al. (2003), Loureiro et al. (2011)]. Few HABs occur during diatom blooms linked to upwelling, whereas most harmful species found are dinoflagellates that are not associated with upwelling but rather events between upwelling episodes. The enhancement of upwelling events in the area caused by climatic alterations would indeed favour the main economic activities in the Sagres region. But, a more detailed study focused on specific harmful algal species and the relation with upwelling processes in the area should be carried out to test this.

5. Conclusions

In response to the research questions in the Introduction, the bio-optical properties of the water column are useful for monitoring phytoplankton blooms along the Southwest Coast of Iberian Peninsula and, furthermore, changes in the phytoplankton community and the bio-optical parameters can be related to the upwelling regime in the area.

Upwelling can be detected not only by lower *in situ* temperatures collected on the day of sampling and favourable wind stress and SST based on upwelling indices, but also by higher coefficients of phytoplankton absorption. Variability in the coloured dissolved fraction of absorption is mostly attributed to influence from the coast, rather than with the phytoplankton dynamics. The findings of this study contribute to a more complete and robust *in situ* database to enable the development and improvement of remote sensing algorithms for primary production.

The contrasting features observed in the Sagres region for phytoplankton biomass and bio-optical properties, highlight the exceptional value of this site for the validation of ocean colour remote sensing data. The historical database and the approach to data acquisition at Sagres could contribute to the future validation of ocean colour sensors such as OLCI, that is part of the ESA Sentinel-3 mission.

It is evident that the use bio-optical parameters for detecting changes in phytoplankton communities in coastal and oceanic waters could provide a cost effective contribution towards environmental monitoring which, in the case of the EU, is centred on the implementation of the WFD, MSFD and MSPD.

Acknowledgements

P.C. Goela and S. Cristina were funded by PhD grants from FCT (SFRH/BD/78356/2011 and SFRH/BD/78354/2011, respectively); J. Icely was funded by EU FP7 AQUA-USERS (grant agreement no. 607325), and EU Horizon 2020 project AquaSpace (grant agreement no. 633576); S. Danchenko was funded by Erasmus Mundus EMJD MACOMA; T. A. DelValls was funded under Bank Santander/UNESCO UNITWIN WiCop; A. Newton was funded by EU FP7 project DEVOTES (grant agreement no. 308392). The data used in this study was acquired under the framework of a project funded by European Space Agency entitled “Technical assistance for the validation of MERIS marine products at Portuguese oceanic and coastal sites” (contract no. 21464/08/I-OL).

We would like to thank Bruno Fragoso and Rodrigo Clímaco, Ricardo and Sara Magalhães for boat and crew support during the sampling campaigns; Kai Sorensen, Merete Grung, Barbro Slide and José Paulo Silva for the technical support with the HPLC-DAD analysis; Sandra Caetano and Cristina Gomes for the phytoplankton counts and Clara Cordeiro, for the help with the time series analysis and decomposition. We also thank the three external reviewers, for their sound advice on improvements to the article.

References

Alvarez, I., Gomez-Gesteira, M., deCastro, M., Dias, J.M., 2008. Spatiotemporal evolution of upwelling regime along the western coast of the Iberian Peninsula. J. Geophys. Res. Oceans 113 (C7). http://dx.doi.org/-10.1029/2008JC004744.

Álvarez-Salgado, X., Labarta, U., Fernández-Reiriz, M., Figueiras, F., Rosón, G., Piedracoba, S., Filgueira, R., Cabanas, J., 2008. Renewal time and the impact of

harmful algal blooms on the extensive mussel raft culture of the Iberian coastal upwelling system (SW Europe). Harmful Algae 7 (6), 849–855.
Alves, J.M., Miranda, P.M., 2012. Variability of Iberian upwelling implied by ERA-40 and ERA-interim reanalyses. Tellus A 65, 19245.
Babin, M., Therriault, J., Legendre, L., Condal, A., 1993. Variations in the specific absorption coefficients for natural phytoplankton assemblages: impact on estimates of primary production. Limnol. Oceanogr. 38 (1), 154–177.
Bakun, A., 1973. Coastal Upwelling Indices, West Coast of North America. Tech. Rep. Technical report NMFS SSRF-671. NOAA.
Bakun, A., 1990. Global climate change and intensification of coastal ocean upwelling. Science 247, 198–201.
Barker, K., 2011. MERIS Optical Measurements Protocols. Part a: in Situ Water Reflectance Measurements. Revision 1.0. Tech. Rep. CO-SCI-ARG-TN-0008.
Beaugrand, G., 2005. Monitoring pelagic ecosystems using plankton indicators. ICES J. Mar. Sci. J. du Conseil 62 (3), 333–338.
Beltrán-Abaunza, J.M., Kratzer, S., Brockmann, C., 2014. Evaluation of MERIS products from baltic sea coastal waters rich in CDOM. Ocean Sci. 10 (3), 377–396.
Blondeau-Patissier, D., Gower, J.F., Dekker, A.G., Phinn, S.R., Brando, V.E., 2014. A review of ocean color remote sensing methods and statistical techniques for the detection, mapping and analysis of phytoplankton blooms in coastal and open oceans. Prog. Oceanogr. 123, 123–144.
Bopp, L., Aumont, O., Cadule, P., Alvain, S., Gehlen, M., 2005. Response of diatoms distribution to global warming and potential implications: a global model study. Geophys. Res. Lett. 32 (19).
Brewin, R.J., Sathyendranath, S., Müller, D., Brockmann, C., Deschamps, P.-Y., Devred, E., Doerffer, R., Fomferra, N., Franz, B., Grant, M., Groom, S., Horseman, A., Hu, C., Krasemann, H., Lee, Z.P., Maritorena, S., Mélin, F., Peters, M., Platt, T., Regner, P., Smyth, T., Steinmetz, F., Swinton, J., Werdell, J., W III, G.N., 2015. The ocean colour climate change initiative: III. A round-robin comparison on in-water bio-optical algorithms. Remote Sens. Environ. 162, 271–294 http://dx.doi.org/10.1016/j.rse.2013.09.016.
Bricaud, A., Stramski, D., 1990. Spectral absorption coefficients of living phytoplankton and nonalgal biogenous matter: a comparison between the Peru upwelling area and the Sargasso Sea. Limnol. Oceanogr. 35, 562–582.
Bricaud, A., Babin, M., Morel, A., Claustre, H., 1995. Variability in the chlorophyll-specific absorption coefficient of natural phytoplankton: analysis and parametrization. J. Geophys. Res. 100 (C7), 13321–13332.
Bricaud, A., Morel, A., Babin, M., Allali, K., Claustre, H., 1998. Variations of light absorption by suspended particles with chlorophyll a concentration in oceanic (case 1) waters: analysis and implications for bio-optical models. J. Geophys. Res. 103, 31033–31044.
Bricaud, A., Claustre, H., Ras, J., Oubelkheir, K., 2004. Natural variability of phytoplanktonic absorption in oceanic waters: influence of the size structure of algal populations. J. Geophys. Res. Oceans 109 (C11). http://dx.doi.org/10.1029/2004JC002419.
Bricaud, A., Babin, M., Claustre, H., Ras, J., Tièche, F., 2010. Light absorption properties and absorption budget of southeast pacific waters. J. Geophys. Res. Oceans 115 (C8).
Casabella, N., Lorenzo, M., Taboada, J., 2014. Trends of the galician upwelling in the context of climate change. J. Sea Res. 93, 23–27.
Ciotti, A.M., Cullen, J.J., Lewis, M.R., 1999. A semi-analytical model of the influence of phytoplankton community structure on the relationship between light attenuation and ocean color. J. Geophys. Res. Oceans 104 (C1), 1559–1578.
Cloern, J.E., Jassby, A.D., 2010. Patterns and scales of phytoplankton variability in Estuarine–coastal ecosystems. Estuaries Coasts 33 (2), 230–241.
Cravo, A., Relvas, P., Cardeira, S., Rita, F., Madureira, M., Sánchez, R., 2010. An upwelling filament off southwest Iberia: effect on the chlorophyll a and nutrient export. Cont. Shelf Res. 30 (15), 1601–1613.
Cristina, S., Goela, P., Icely, J., Newton, A., Fragoso, B., 2009. Assessment of water-leaving reflectance of oceanic and coastal waters using MERIS satellite products off the southwest coast of Portugal. J. Coast. Res. SI 56, 1479–1483.
Cristina, S.C.V., Moore, G.F., Goela, P.R.F.C., Icely, J.D., Newton, A., 2014. In situ validation of MERIS marine reflectance off the southwest Iberian Peninsula: assessment of vicarious adjustment and corrections for near-land adjacency. Int. J. Remote Sens. 35 (6), 2347–2377.
Cristina, S., Icely, J., Goela, P., DelValls, T., Newton, A., 2015. Using remote sensing as a support to the implementation of the European marine strategy framework directive in SW Portugal. Cont. Shelf Res. (in press) http://dx.doi.org/10.1016/j.csr.2015.03.011.
Cropper, T.E., Hanna, E., Bigg, G.R., 2014. Spatial and temporal seasonal trends in coastal upwelling off Northwest Africa, 1981–2012. Deep-sea Res. I 86, 94–111.
Cullen, J.J., 2008. Real-time Coastal Observing Systems for Marine Ecosystem Dynamics and Harmful Algal Blooms. In: Observation and Prediction of Harmful Algal Blooms. UNESCO Publishing, France, Ch, pp. 1–41.
David, V., Ryckaert, M., Karpytchev, M., Bacher, C., Arnaudeau, V., Vidal, N., Maurer, D., Niquil, N., 2012. Spatial and long-term changes in the functional and structural phytoplankton communities along the French Atlantic coast. Estuar. Coast. Shelf Sci. 108 (0), 37–51.
Devlin, M., Best, M., Coates, D., Bresnan, E., O'Boyle, S., Park, R., Silke, J., Cusack, C., Skeats, J., 2007. Establishing boundary classes for the classification of UK marine waters using phytoplankton communities. Mar. Pollut. Bull. 55, 91–103.
Devlin, M., Barry, J., Painting, S., Best, M., 2009. Extending the phytoplankton tool kit for the UK Water framework directive: indicators of phytoplankton community structure. Hydrobiologia 633 (1), 151–168.
Doerffer, R., 2002. Protocols for the Validation of MERIS Water Products. Tech. Rep. PO-TN-MEL-GS-0043. European Space Agency.
Doerffer, R., Schiller, H., 2007. The MERIS case 2 water algorithm. Int. J. Remote Sens. 28 (3–4), 517–535.
Domingues, R.B., Barbosa, A., Galvão, H., 2008. Constraints on the use of phytoplankton as a biological quality element within the water framework directive in Portuguese waters. Mar. Pollut. Bull. 56 (8), 1389–1395.
Directive 2000/60/EC of the European parliament and of the council of 23 october 2000 establishing a framework for community action in the field of water policy. Off. J. Eur. Union, 2000. L 327/1.
Directive 2008/56/EC of the European parliament and of the council of 17 june 2008 establishing a framework for community action in the field of marine environmental policy (marine strategy framework directive). Off. J. Eur. Union, 2008. L 164/19.
Edwards, V., Icely, J., Newton, A., Webster, R., 2005. The yield of chlorophyll from nitrogen: a comparison between the shallow Ria Formosa lagoon and the deep oceanic conditions at sagres along the southern coast of Portugal. Estuar. Coast. Shelf Sci. 62 (3), 391–403.
Directive 2014/89/EU of the European parliament and of the council of 23 July 2014 establishing a framework for maritime spatial planning. Official J. Eur. Union, 2014. L 257/135.
Evans, J., 1972. A modified sedimentation system for counting algae with an inverted microscope. Hydrobiology 40, 247–250.
Ferrari, G., Tassan, S., 1999. A method using chemical oxidation to remove light absorption by phytoplankton pigments. J. Phycol. 35, 1090–1098.
Ferreira, A., Garcia, V.M., Garcia, C.A., 2009. Light absorption by phytoplankton, non-algal particles and dissolved organic matter at the patagonia shelf-break in spring and summer. Deep Sea Res. Part I Oceanogr. Res. Pap. 56 (12), 2162–2174.
Fiúza, A.F.G., Macedo, M.A., Guerreiro, M.R., 1982. Climatological space and time variations of the Portuguese coastal upwelling. Oceanol. Acta 5, 31–40.
Garmendia, M., Ángel Borja, Franco, J., Revilla, M., 2013. Phytoplankton composition indicators for the assessment of eutrophication in marine waters: present state and challenges within the European directives. Mar. Pollut. Bull. 66, 7–16.
Gibb, S.W., Cummings, D.G., Irigoien, X., Barlow, R.G., Fauzi, R., Mantoura, C., 2001. Phytoplankton pigment chemotaxonomy of the northeastern Atlantic. Deep Sea Res. Part II Top. Stud. Oceanogr. 48 (4–5), 795–823.
Goela, P.C., Icely, J., Cristina, S., Newton, A., Moore, G., Cordeiro, C., 2013. Specific absorption coefficient of phytoplankton off the Southwest coast of the Iberian Peninsula: a contribution to algorithm development for ocean colour remote sensing. Cont. Shelf Res. 52, 119–132.
Goela, P., Danchenko, S., Icely, J., Lubian, L., Cristina, S., Newton, A., 2014. Using CHEMTAX to evaluate seasonal and interannual dynamics of the phytoplankton community off the south-west coast of Portugal. Estuar. Coast. Shelf Sci. 151 (0), 112–123.
Gordon, H.R., Clark, D.K., Brown, J.W., Brown, O.B., Evans, R.H., Broenkow, W.W., Jan 1983. Phytoplankton pigment concentrations in the middle Atlantic bight: comparison of ship determinations and CZCS estimates. Appl. Opt. 22 (1), 20–36.
Hu, C., Sathyendranath, S., Shutler, J.D., Brown, C.W., Moore, T.S., Craig, S.E., Soto, I., Subramaniam, A., 2014. Phytoplankton Functional Types from Space. No. 15. In: Detection of Dominant Algal Blooms by Remote Sensing. IOCCG, Dartmouth, Cananda, Ch, pp. 39–70.
Johnsen, G., Volent, Z., Tangen, K., Sakshaug, E., 1997. Monitoring Algal Blooms: New Technologies for Detecting Large-scale Environmental Change. In: Time Series of Harmful and Benign Phytoplankton Blooms in Northwest European Waters Using the Seawatch Buoy System. Landes Bioscience, Ch, pp. 115–143.
Kifani, S., Masski, H., Faraj, A., 2008. The need of an ecosystem approach to fisheries: the Moroccan upwelling-related resources case. Fish. Res. 94 (1), 36–42.
Kutser, T., 2009. Passive optical remote sensing of cyanobacteria and other intense phytoplankton blooms in coastal and inland waters. Int. J. Remote Sens. 30 (17), 4401–4425.
Lemos, R.T., Pires, H.O., 2004. The upwelling regime off the west Portuguese coast, 1941-2000. Int. J. Climatol. 24 (4), 511–524.
Lemos, R.T., Sansó, B., 2006. Spatio-temporal variability of ocean temperature in the Portugal current system. J. Geophys. Res. Oceans 111 (C4). http://dx.doi.org/10.1029/2005JC003051.
Leterme, S., Pingree, R., Skogen, M., Seuront, L., Reid, P., Attrill, M., 2008. Decadal fluctuations in North Atlantic water inflow in the North sea between 1958-2003: impacts on temperature and phytoplankton populations. Oceanologia 50 (1), 59–72.
Lorenzo, E.D., Miller, A., Schneider, N., McWilliams, J., 2005. The warming of the California current system: dynamics and ecosystem implications. J. Phys. Oceanogr. 35, 336–362.
Loureiro, S., Newton, A., Icely, J., 2005. Microplankton composition, production and upwelling dynamics in Sagres (SW Portugal) during the summer of 2001. Sci. Mar. 69 (3), 323–341.
Loureiro, S., Icely, J., Newton, A., 2008. Enrichment experiments and primary production at sagres (SW Portugal). J. Exp. Mar. Biol. Ecol. 359 (2), 118–125.
Loureiro, S., Reñé, A., Garcés, E., Camp, J., Vaqué, D., 2011. Harmful algal blooms (HABs), dissolved organic matter (DOM), and planktonic microbial community dynamics at a near-shore and a harbour station influenced by upwelling (SW Iberian Peninsula). J. Sea Res. 65 (4), 401–413.
Lyon, P.E., Hoge, F.E., Wright, C.W., Swift, R.N., Yungel, J.K., Nov 2004. Chlorophyll biomass in the global oceans: satellite retrieval using inherent optical properties. Appl. Optics 43 (31), 5886–5892.
Mackey, M., Mackey, D., Higgins, H., Wright, S., 1996. CHEMTAX – a program for

estimating class abundances from chemical markers: application to HPLC measurements of phytoplankton. Mar. Ecol. Prog. Ser. 114, 265–283.
Margalef, R., 1978. Life-forms of phytoplankton as survival alternatives in an unstable environment. Oceanol. Acta 1, 493–509.
Mendes, C.R., Sá, C., Vitorino, J., Borges, C., Garcia, V.M.T., Brotas, V., 2011. Spatial distribution of phytoplankton assemblages in the nazaré submarine canyon region (Portugal): HPLC-CHEMTAX approach. J. Mar. Syst. 87 (1), 90–101.
Millán-Nuñez, E., Sieracki, M.E., Millán-Nuñez, R., Lara-Lara, J.R., Gaxiola-Castro, G., Trees, C.C., 2004. Specific absorption coefficient and phytoplankton biomass in the southern region of the California current. Deep Sea Res. Part II Top. Stud. Oceanogr. 51 (6–9), 817–826.
Mitchell, G., A, A.B., Carder, K., Cleveland, J., Ferrari, G., Gould, R., Kahru, M., Kishino, M., Maske, H., Moisan, T., Moore, L., Nelson, N., Phimney, D., Reynodls, R., Sosik, H., Stramski, D., Tassan, S., Trees, C., Weideman, A., Wieland, J., Vodacek, A., 2000. Ocean Optics Protocols for Satellite Ocean Colour Sensor Validation, Revision 2. NASA Tech. Memo. 209966. In: Determination of Spectral Absorption Coefficients of Particles, Dissolved Material and Phytoplankton for Discrete Water Samples. NASA Goddard Space Flight Center, Greenbelt, Maryland, Ch, pp. 125–153.
Mueller, J., Austin, R., 1995. Ocean Optics Protocols for SeaWiFS Validation, Revision 1, vol. 25. NASA Goddard Space Flight Center, Greenbelt, Maryland.
O'Reilly, J.E., Maritorena, S., Mitchell, B.G., Siegel, D.A., Carder, K.L., Garver, S.A., Kahru, M., McClain, C.R., 1998. Ocean color chlorophyll algorithms for seawifs. J. Geophys. Res. 103, 24937–24953.
Palma, A.S., Vilarinho, M.G., Moita, M.T., 1998. Interannual trends in the longshore variation of dinophysis off the Portuguese coast. In: Reguera, B., Blanco, J., Fernández, M.L., Wyatt, T. (Eds.), Proc. VIII Int. Conf. Harmful Algae. Xunta de Galicia and IOC-UNESCO, Vigo, pp. 124–127.
Pegau, W., Zaneveld, J., 1993. Temperature-dependent absorption of water in the red and near-infrared portions of the spectrum. Limnol. Oceanogr. 38, 188–192.
Peliz, A.J., Fiúza, A.F.G., 1999. Temporal and spatial variability of CZCS-derived phytoplankton pigment concentrations off the western Iberian Peninsula. Int. J. Remote Sens. 20 (7), 1363–1403.
Preisendorfer, R.W., 1971. General theory of radiative transfer across the random atmosphere-ocean interface. J. Quant. Spectrosc. Radiat. Transf. 11 (6), 723–737.
R Core Team, 2015. R: a Language and Environment for Statistical Computing. R Foundation for Statistical Computing, Vienna, Austria. http://-www.R-project.org/.
Ramos, A.M., Pires, A.C., Sousa, P.M., Trigo, R.M., 2013. The use of circulation weather types to predict upwelling activity along the western Iberian Peninsula coast. Cont. Shelf Res. 69, 38–51.
Reguera, B., Garcés, E., Pazos, Y., Bravo, I., Ramilo, I., González-Gil, S., 2003. Cell cycle patterns and estimates of in situ division rates of dinoflagellates of the genus dinophysis by a postmitotic index. Mar. Ecol. Prog. Ser. 249, 117–131.
Relvas, P., Barton, E., 2002. Mesoscale patterns in the Cape São Vicente (Iberian Peninsula) upwelling region. J. Geophys. Res. Oceans 107, 3164.
Reynolds, R., Smith, T., Liu, C., Chelton, D., Casey, K., Schlax, M., 2007. Daily high-resolution blended analyses for sea surface temperature. J. Clim. 20, 5473–5496.
Rueda-Roa, D.T., Muller-Karger, F.E., 2013. The southern Caribbean upwelling system: sea surface temperature, wind forcing and chlorophyll concentration patterns. Deep Sea Res. Part I Oceanogr. Res. Pap. 78, 102–114.
Sathyendranath, S., 2000. Remote Sensing of Ocean Colour in Coastal, and Other Optically-complex, Waters. IOCCG Report Number 3. IOCCG.
Schlüter, L., Møhlenberg, F., Havskum, H., Larsen, S., 2000. The use of phytoplankton pigments for identifying and quantifying phytoplankton groups in coastal areas: testing the influence of light and nutrients on pigment/chlorophyll a ratios. Mar. Ecol. Prog. Ser. 192, 49–63.
Smith, S.V., Hollibaugh, J.T., 1993. Coastal metabolism and the oceanic organic carbon balance. Rev. Geophys. 31 (1), 75–89.
Smith, M.E., Bernard, S., O'Donoghue, S., 2013. The assessment of optimal MERIS ocean colour products in the shelf waters of the KwaZulu-natal bight, South Africa. Remote Sens. Environ. 137, 124–138.
Sousa, F.M., Bricaud, A., 1992. Satellite-derived phytoplankton pigment structures in the Portuguese upwelling area. J. Geophys. Res. Oceans 97 (C7), 11343–11356.
Tangen, K., 1997. Monitoring phytoplankton blooms continuously with seawatch technology. In: Stel, J.H., Behrens, H.W.A., J.B., L.D. , van der Meulen, J. (Eds.), Proceedings of the First International Conference on EuroGOOS, Vol. 62 of Elsevier Oceanography Series. Elsevier, pp. 539–546.
Tassan, S., Ferrari, G., 1995. An Alternative approach to absorption measurements of aquatic particles retained on filters. Limnol. Oceanogr. 40, 1358–1368.
Tassan, S., Ferrari, G., 2002. A sensitivity analysis of the "transmittance-reflectance" method for measuring light absorption by aquatic particles. J. Plankton Res. 24 (8), 757–774.
Tilstone, G.H., Moore, G.F., Sørensen, K., Doerffer, R., Røttgers, R., Ruddick, K.G., Pasterkamp, R., Jørgensen, P., 2002. REVAMP - Regional Validation of MERIS Chlorophyll Products in North Sea Coastal Waters - Protocols Document. Tech. Rep. EVG1 – CT –; 2001–00049.
Utermöhl, V., 1931 (Mit besondere Beriicksichtigung des Ultraplanktons). Verhandlungen. Neue Wege in der quantitativen Erfassung des Planktons, 5. Internationale Vereinigung fur Theoretische und Angewandte Limnologie, pp. 567–595.
Vantrepotte, V., Brunet, C., Mériaux, X., Lécuyer, E., Vellucci, V., Santer, R., 2007. Bio-optical properties of coastal waters in the Eastern english channel. Estuar. Coast. Shelf Sci. 72, 201–212.
Wright, S., Jeffrey, S., 1997. Phytoplankton Pigments in Oceanography. In: High-resolution HPLC System for Chlorophylls and Carotenoids of Marine Phytoplankton. UNESCO Publishing, Ch, pp. 327–341.
Yentsch, C.S., 1968. Measurement of visible light absorption by particulate matter in the ocean. Limnol. Oceanogr. 7, 207–217.
Yentsch, C.S., Phinney, D.A., 1989. A bridge between ocean optics and microbial ecology. Limnol. Oceanogr. 34, 1694–1705.
Zhang, H.-M., Reynolds, R.W., Bates, J.J., 2006. Blended and gridded high resolution global sea surface wind speed and climatology from multiple satellites: 1987 – Present. In: American Meteorological Society 2006 Annual Meeting, Paper P2.23, Atlanta, GA, January 29 – February 2.